

<https://doi.org/10.1038/s42003-025-08639-y>

Multiplexed bacteriocin synthesis to combat and prevent antimicrobial resistance



Alex Quintero-Yanes¹✉, Kenny Petit¹, Hector Rodriguez-Villalobos², Hanne Vande Capelle^{3,4}, Olivier De Veirman¹, Hans Gerstmans^{3,4}, Joleen Masschelein^{3,4}, Juan Borrero⁵, Pascal Hols⁶ & Philippe Gabant¹✉

Bacteriocins are underexplored yet promising candidates to combat antimicrobial resistance (AMR) and enable targeted therapy due to their natural origin, abundance and narrow spectrum of activity. In this study, we used a collection of engineered DNA devices and cell-free gene expression (CFE) to rapidly produce combinations (cocktails) of bacteriocins comprising both linear and circular proteins. Other cocktails were designed to target a specific bacterial species by leveraging insights into bacteriocin pathways for cell envelope penetration. These tailored combinations eradicated bacteria effectively while preventing resistance development. The synthesis of bacteriocins was optimized by using continuous exchange CFE, reengineering DNA parts, and adjusting conditions for disulfide bond formation. Also, we illustrate the efficacy of these bacteriocin mixtures against various multidrug-resistant human pathogens and highlight their potential through in vivo testing in the animal model *Galleria mellonella*. Our bacteriocin cocktail expression and test platform underscores the potential of bacteriocins for innovative treatments against multidrug-resistant infections.

Bacteriocins, a unique class of naturally occurring antimicrobial peptides (AMPs) produced by bacteria, offer a distinctive solution in the fight against bacterial infections¹. These molecules display both broad- and narrow-spectrum activity but typically target bacteria more selectively than traditional antibiotics. Bacteriocin-based therapies therefore have the potential to specifically target pathogenic bacteria while minimizing disruptions to the microbiota^{2–5}.

Cell-free synthetic biology is emerging as a powerful tool for simplifying AMP synthesis and assessing their therapeutic potential. Previously, we developed the PARAGEN collection, a curated repository of bacterial DNA sequences engineered for cell-free expression (CFE), to produce both linear and circular bacteriocins^{6,7} (Fig. 1). This collection enables rapid screening, allowing bacteriocin production to be completed within 2–3 h and activity assessments on bacterial lawns within a day (6–12 h) (Fig. 1). CFE of the PARAGEN genes has been instrumental in elucidating mechanisms of bacteriocin activity against human pathogenic bacteria^{8,9}. Moreover, CFE coupled with de novo coding sequences designed with deep learning models facilitated the parallelized synthesis of short AMPs with broad-spectrum of activity¹⁰.

Probiotic engineering further expands the application of bacteriocins to control bacterial communities¹¹. Recently, non-pathogenic *Escherichia coli* strains have been genetically modified to secrete bacteriocins targeting specific pathogenic bacteria, such as *Enterococcus faecium* and enterohemorrhagic *E. coli*^{12,13}. However, it is important to note that despite the concerted production of bacteriocins, pathogens eventually develop resistance, allowing them to outcompete the probiotic strains over time¹².

The strategic use of antimicrobial combinations, or cocktails, represents a significant advancement in combatting bacterial infections¹⁴. Combinations of bacteriocins with either antibiotics or phages have shown promising results against pathogenic bacteria^{15–17}. Cocktails composed solely of bacteriocins can also efficiently control bacteria^{18,19}. Traditionally, bacteriocin cocktails have relied on peptides synthesized chemically or proteins produced in vivo through ectopic gene expression and subsequent purification from bacterial pellets or culture supernatants. While traditional production methods involve chemical synthesis or biosynthesis, these approaches can be laborious and time-consuming. In contrast, CFE offers a faster and more efficient alternative^{20,21}.

¹Syngulon SA, Seraing, Belgium. ²Microbiology Department, Cliniques Universitaires Saint-Luc, Université Catholique de Louvain (UCLouvain), Brussels, Belgium. ³VIB-KU Leuven Center for Microbiology, Flanders Institute for Biotechnology, Leuven, Belgium. ⁴Department of Biology, KU Leuven, Leuven, Belgium. ⁵Sección Departamental de Nutrición y Ciencia de los Alimentos, Facultad de Veterinaria, Universidad Complutense de Madrid (UCM), Madrid, Spain. ⁶Louvain Institute of Biomolecular Science and Technology, Université Catholique de Louvain, Louvain-la-Neuve, Belgium. ✉e-mail: aquintero@syngulon.com; pgabant@gmail.com

Here, we aimed to multiplex bacteriocin synthesis in single CFE reactions to enable robust and rapid production of antimicrobial cocktails. By considering the pathways by which bacteriocins cross the cell envelope,

we designed cocktails that can synergistically kill bacteria and prevent resistance. A second set of cocktails, comprising bacteriocins of different sizes and structures, showed an expanded spectrum of activity, targeting

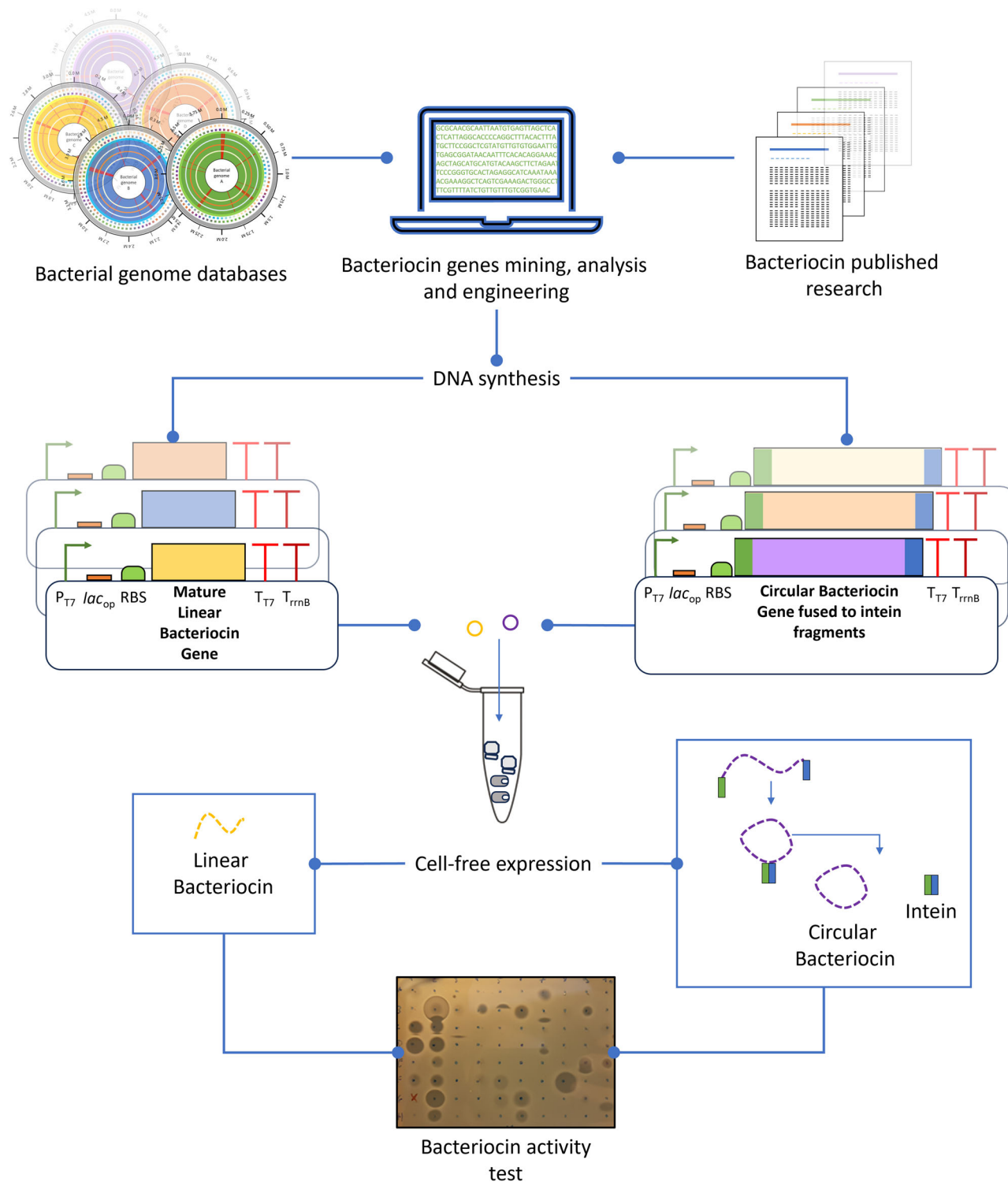


Fig. 1 | Bacteriocin in vitro genetic expression with the PARAGEN collection. Bacteriocin expression devices are engineered for CFE using synthetic biology approaches, such as abstraction, standardization, modularization, and optimization. Genes coding for bacteriocin peptides and proteins are searched in bacterial genome databases and published research. Genetic parts coding for coding for either linear or circular bacteriocins are optimized in silico for codon usage and synthesized de novo together with standardized genetic parts, such as the T7 RNA polymerase promoter (P_{T7}), ribosome binding site (RBS), and transcription terminators (T₇ and T_{rrnB}).

Only the coding sequence for the mature peptide is integrated in the genetic module, while for circular peptides, bacteriocin genes are fused with intein fragments for circularization. The bacteriocin expression devices are cloned into multi-copy vectors that can be transformed in *E. coli* for pDNA replication. A lac operator (*lac_{op}*) is included to repress leaky expression while plasmids are carried in *E. coli* and, thus, avoid toxicity by bacteriocin expression. Synthesis takes 2–3 h in vitro with conventional CFE kits. Thereafter, bacteriocins are tested on high-density bacterial cell lawns in their respective standard growth media and conditions.

Table 1 | Bacteriocins produced in this study by CFE with pDNA from the PARAGEN collection

Bacteriocin name	Abbreviation	Structure type	Bacterial target	Reference
Colicin M	ColM	Linear unmodified	<i>E. coli</i>	22
Colicin E1	ColE1	Linear unmodified	<i>E. coli</i>	22
Enterocin L50A	EntL50A	Linear unmodified	<i>Pediococcus pentosaceus</i> and <i>Lactococcus lactis</i>	50
Garvicin ML	GarML	Circular	<i>Pediococcus pentosaceus</i> and <i>Lactococcus lactis</i>	7
Microcin L	MccL	Linear with DSB	<i>E. coli</i>	22,23
Microcin V (Colicin V)	MccV	Linear with DSB	<i>E. coli</i>	22,23
Salmonicin E1B	SalE1B	Linear unmodified	<i>E. coli</i> and <i>Salmonella</i> species	25

both Gram-positive and -negative bacteria. Our work provides a foundation for developing targeted antimicrobial strategies that can be rapidly tested in vitro and in vivo, addressing the urgent challenges posed by the growing pressure of antimicrobial resistance (AMR) on healthcare systems.

Results

Rational design of bacteriocin cocktails to enhance antimicrobial potency

To enable co-expression of bacteriocins in a single reaction, we used CFE in combination with different bacteriocin DNA templates from the PARAGEN collection (Table 1). First, we tested whether two bacteriocins targeting the same bacterial species could improve killing efficacy (i.e., in terms of synergy and AMR prevention). We selected *E. coli* strains for these experiments, as the mechanisms underlying the activity of different bacteriocins have been extensively elucidated in this enterobacterial pathogen^{22,23}. Sensitivity to bacteriocins in *E. coli* hinges on the functionality of transport and structural proteins in the inner and outer membranes (Fig. 2A). Outer membrane porins exhibit lower specificity compared to inner membrane proteins^{22,23}. These porins rely on the Ton or Tol systems for their proper functioning and interaction with bacteriocins^{22,23}. Consequently, single mutations in porins or Ton/Tol genes can confer pleiotropic resistance (cross-resistance) against multiple bacteriocins.

We investigated the CFE of different bacteriocin combinations, including microcins, colicins, and colicin-like bacteriocins, to assess their bactericidal activity and ability to prevent resistance development (Table 1). First, we confirmed the activity of ColM, SalE1B, MccV, and MccL by complementing mutants from the Keio collection²⁴ with specific cell envelope receptor genes (Fig. 2A and Supplementary Fig. 1a). Although receptor and transporter genes for SalE1B have not been determined experimentally, we predicted that SalE1B to be a BtuB-TolC-TolA-dependent bacteriocin based on its homology to ColE1²⁵ (Fig. 2A). Indeed, we could confirm that SalE1B depends on TolC for activity on *E. coli* (Supplementary Fig. 1a).

We also noticed that CFE of SalE1B rendered a higher activity than ColE1 against *E. coli* BW25113, as demonstrated by the activity of the serially diluted bacteriocins (Supplementary Fig. 1b, c). Other bacteriocins, such as ColM and MccL, retained their activity after serial dilutions, while MccV did not (Supplementary Fig. 1b, c). Consequently, we prepared bacteriocin combinations of SalE1B, ColM, and MccL using CFE.

Bacterial growth was first monitored upon treatment with individually expressed bacteriocins. After overnight incubation, colonies emerged within the inhibition zones, and growth resumed in liquid cultures after a six-hour arrest (Fig. 2B, C). This observation indicated that resistance rapidly developed within some cells in the single bacteriocin-treated cultures. Further characterization of the colonies within the SalE1B-derived halo revealed that the isolates were less sensitive or fully resistant to SalE1B, compared to the parental strain *E. coli* BW25113, and mutations in genes associated with the colicin E1 homologous pathway, such as *btuB*, *tolC*, and *tolA* were detected (Supplementary Fig. 2a and Supplementary Table 1). Sensitivity to SalE1B could be restored in one of the isolates displaying complete resistance (mutant # 7) and carrying the mutation *tolC*_{Q347*} through complementation with *tolC* from the parental strain

(Supplementary Fig. 2b). Surprisingly, we also detected *fhuA* mutations in some isolates, which is associated with TonB-dependent bacteriocins. Given that knocking out *fhuA* does not confer resistance to SalE1B (Supplementary Fig. 1c), we can rule out the possibility of FhuA being essential for SalE1B activity.

Notably, we observed that treatment with cocktails of bacteriocins that utilize distinct pathways to cross the cell envelope (ColM + SalE1B and MccL + SalE1B) did not result in resistance development (Fig. 2B, C). Viability assays conducted on cells grown in liquid cultures further confirmed that ColM + SalE1B and MccL + SalE1B effectively eradicated the cells after 72 h (Fig. 2D). In contrast, when cultures were treated with ColM + MccL, which both rely on the TonB-dependent pathway, colonies appeared within the inhibition zone (Fig. 2B, red arrows). In addition, growth was observed in liquid culture, although it appeared later compared to single bacteriocin treatment, and viable cells were detected (Fig. 2B–D). This underscores the importance of considering receptor redundancy and transport pathways (rational design) in bacteriocin cocktail preparations for mitigating resistance development.

To assess synergistic effects, we diluted the single and co-expressed bacteriocin solutions over a 1000-fold and tested their activity against cultures of *E. coli* BW25113 (Fig. 2E). Consistent with the results on solid media, MccL was not efficient in killing bacteria in such dilutions, while SalE1B and especially ColM, showed better activities compared to untreated control cultures. Notably, the cocktails ColM + SalE1B and MccL + SalE1B showed enhanced bactericidal activities compared to their individually synthesized counterparts, indicating that the co-expressed bacteriocins have a synergistic effect.

Re-engineering of bacteriocin synthesis for improved cocktail activity

As observed above, ColE1 and MccV showed poor activity compared to ColM, MccL, and SalE1B (Supplementary Fig. 1b). To improve bacteriocin CFE, we redesigned the bacteriocin genes using DNA template optimization guidelines for CFE from PureFrex (GeneFrontier Corporation). We also explored the removal of the *lac* operator from our original bacteriocin expression devices, as a recent report showed that this can further enhance protein yield in CFE systems²⁶. To evaluate this combined optimization strategy, we first measured GFP expression, observing a tenfold increase in fluorescence with the optimized expression device (Fig. 3A). Testing ColE1 activity confirmed that adjustments to the gene sequence and removal of the *lac* operator independently and synergistically enhanced bacteriocin expression (Fig. 3B). Consequently, we re-engineered the original PARAGEN *mccV* device and tested its synthesis. MccV from this optimized DNA template could be detected in samples diluted over 200-fold compared to the original device (Fig. 3C).

Given that MccV is predicted to form disulfide bonds (DSB) in nature²⁷, we tested its synthesis using commercially available supplements designed to enhance DSB formation in CFE systems. The addition of these supplements led to a twofold increase in MccV activity when using the optimized device (Fig. 3C).

Considering that ColE1 and MccV use different receptors and pathways to cross the cell envelope (Fig. 2A), we co-expressed them and assessed

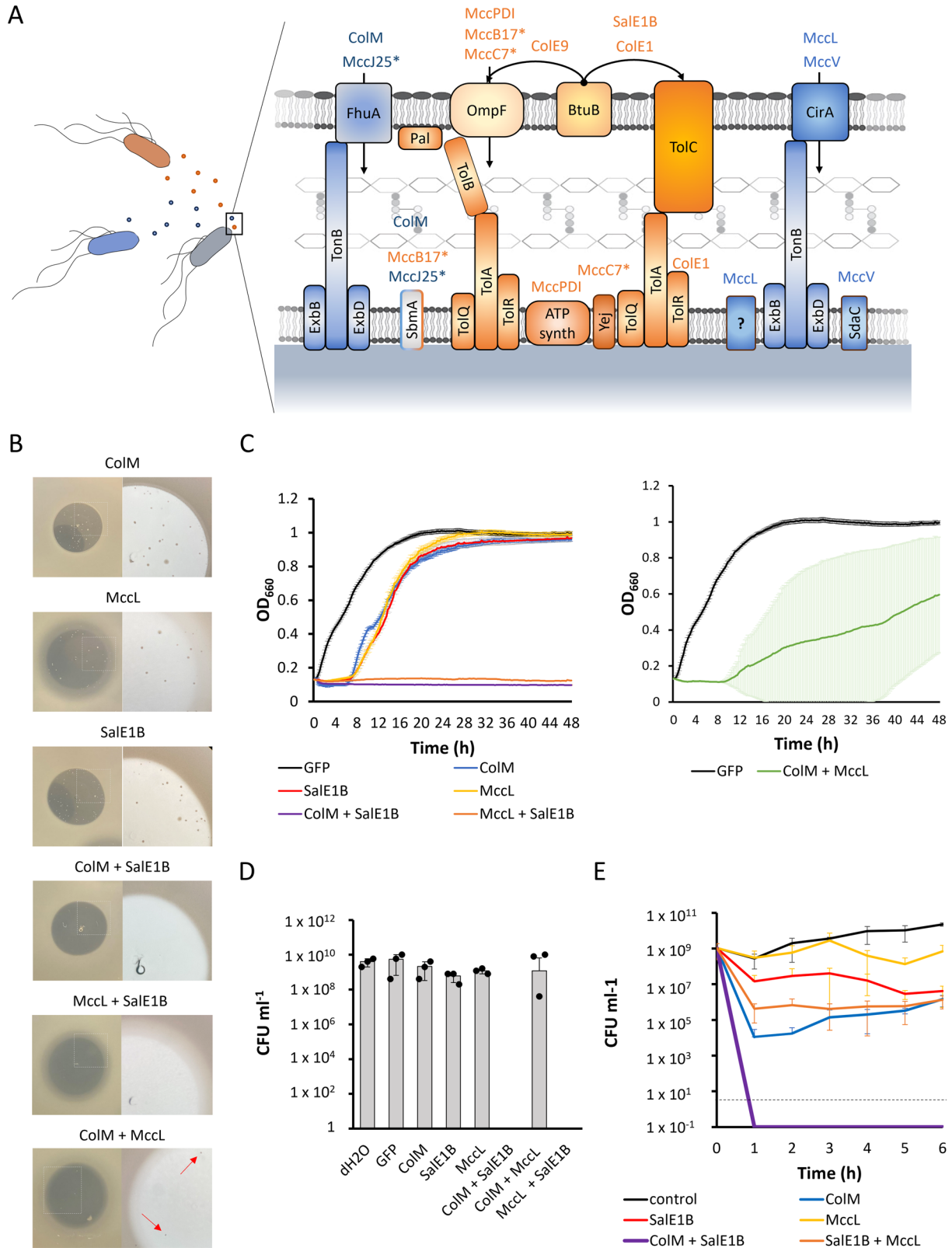


Fig. 2 | Rational designed and cell-free expressed bacteriocin cocktail.

A Bacteriocins pathways in *E. coli* cell envelope. Tol and Ton-dependent bacteriocin pathways are highlighted in orange and blue, respectively, as well as producer cells and bacteriocins targeting those pathways. Different colicins and microcins are distinguished with the Col and Mcc prefixes, respectively, while post-translationally modified bacteriocins are indicated with an asterisk (*). **B** Activity of different bacteriocins against *E. coli* BW25113. Halo of activity as seen by the naked eye (left)

and under a stereo microscope to detail colonies appearing in the halos (right). **C** Growth (OD_{600}) of *E. coli* BW25113 in liquid cultures supplemented with single and co-expressed bacteriocins. **D** Viability ($CFU\ ml^{-1}$) of cells in cultures (from C) after 72 h. **E** CFU counts of *E. coli* BW25113 in liquid cultures supplemented with single and co-expressed bacteriocins 1250-fold diluted. Lines in (C and E) and bars in (D) represent the average of three biological replicates \pm SD. Dots in (D) show the values of replicates.

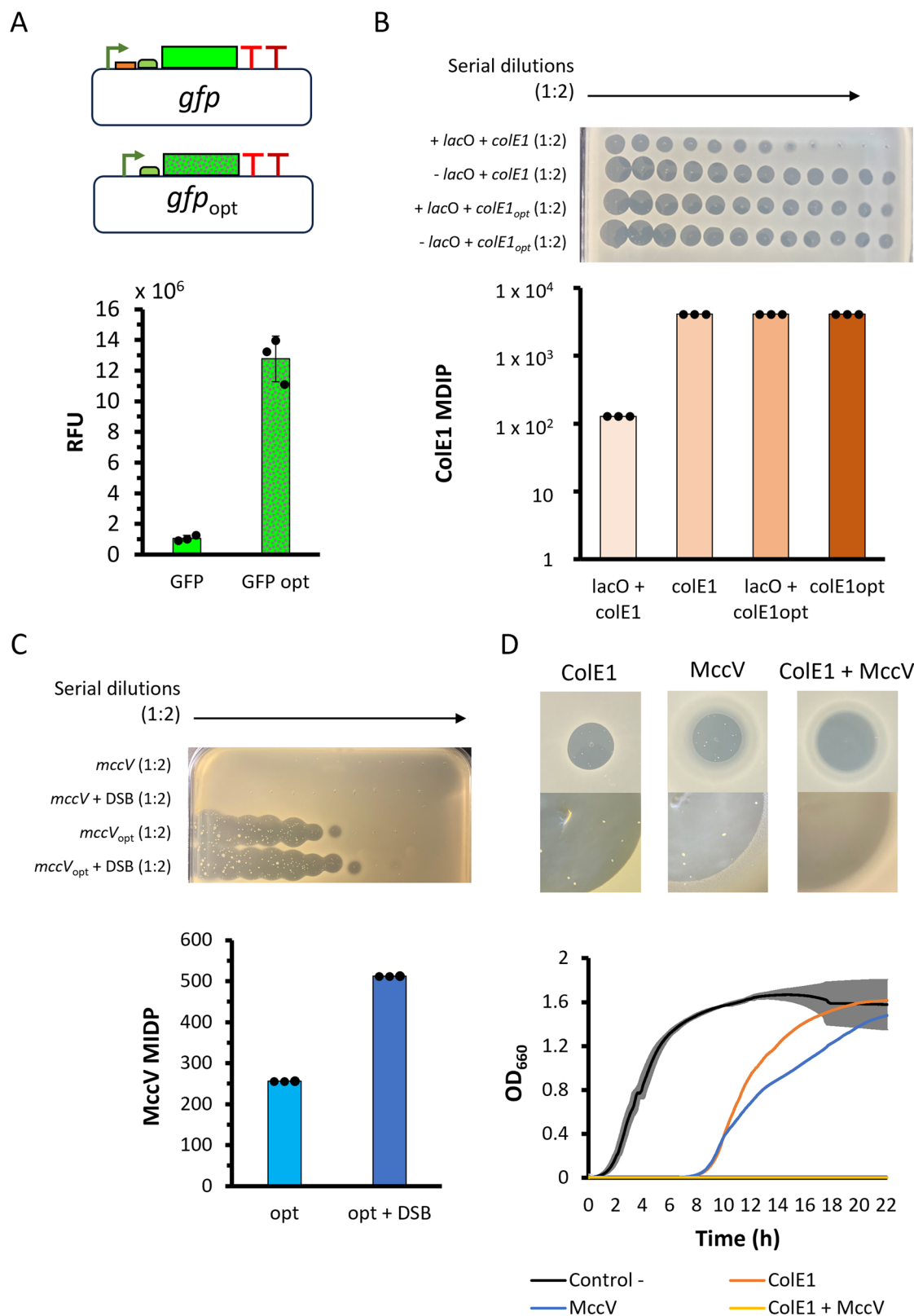


Fig. 3 | Optimization of PARAGEN sequences increase bacteriocin activity.

A Gene expression devices for CFE of GFP with and without optimization (gfp_{opt} , green box, and gfp , dotted box, respectively). Measurement (RFU) of CFE of GFP devices. **B, C** Activity of ColE1 (**B**) and MccV (**C**) from CFE with and without optimization as seen against a top law of *E. coli* BW25113 and after measuring the MDIP. **B** Impact on ColE1 activity with the original PARAGEN device (+lacO + colE1), after removing either the lac operator (-lacO + colE1), after optimizing the codon usage of a bacteriocin gene (+lacO + colE1_{opt}) or in combining both

optimization strategies (-lacO + colE1_{opt}). **C** Activity of MccV with or without optimization in presence or absence of supplements for disulfide bond formation (DSB) against a top law of *E. coli* BW25113, and minimum inhibitory dilution as seen on plates (MIDP) of CFE MccV optimized without and with a DSB supplement. **D** Activity on plates and liquid cultures of single and cocktail CFE of ColE1 and MccV with a DSB supplement. Bars (in **A–C**) and lines (**D**) are representative of the average value of three technical replicates (**A**) and the activity on three biological replicates, ± SD (in **B–D**). Dots in (**A–C**) show the values of replicates.

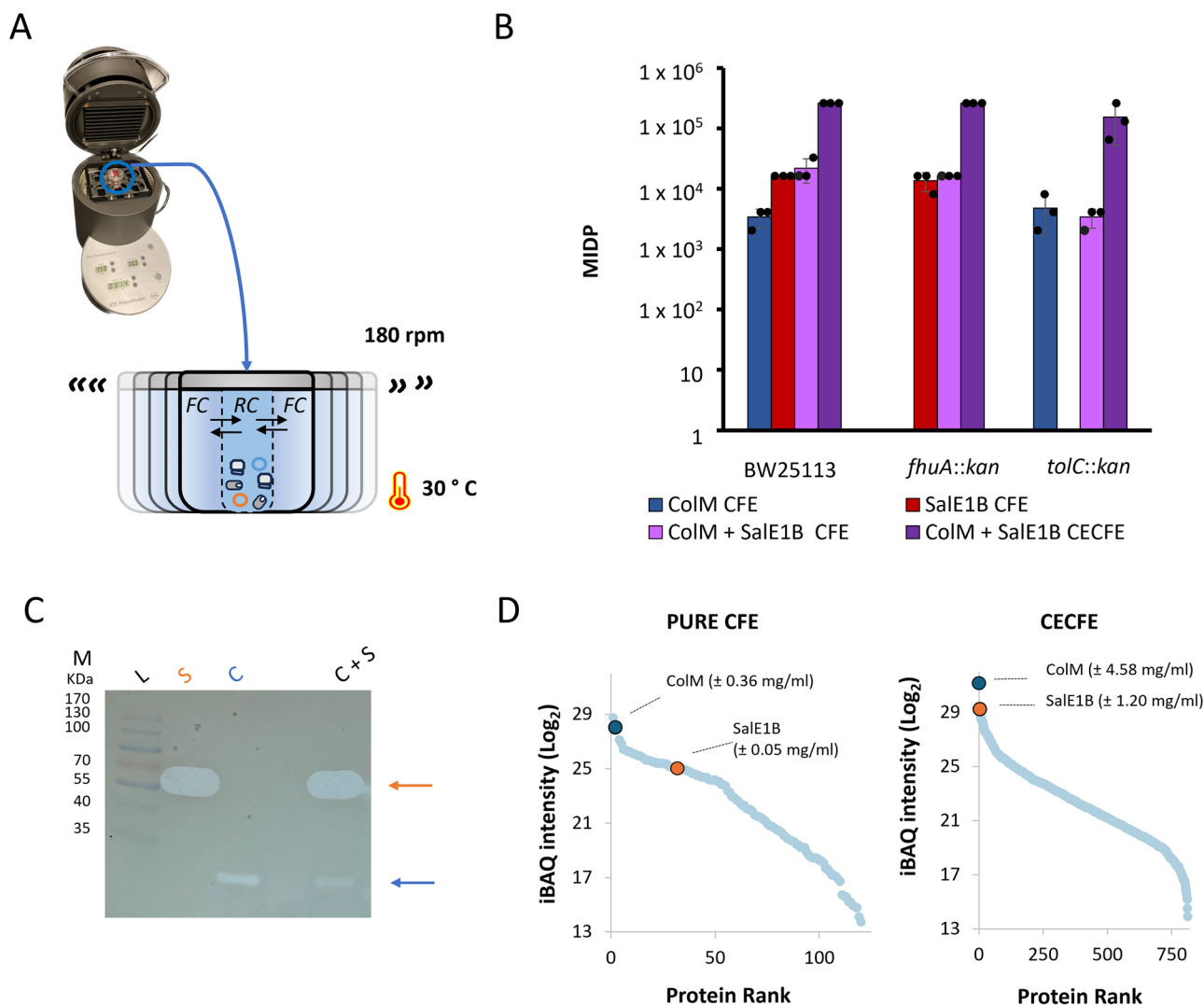


Fig. 4 | CECFE scaling up and de-multiplexing bacteriocins in cocktail.

A Diagram of synthesis of the ColM + SalE1B cocktail with CEFCE using the RTs ProteoMaster Instrument (Roche). The feeding chamber (FC) contains substrates and energy cofactors, while the reaction chamber (RC) holds the pDNA, and transcription and translation machinery. Reactions are shaken (180 rpm) to improve diffusion of substrates into RC and of byproducts of protein synthesis out to FC. **B** MIDP of cocktail preparations using PURE CFE (PCFE) and CECFE reactions. **C** The activity of each bacteriocin in the cocktail was distinguished following separation by molecular weight with Tris-Tricine SDS-page and test of activity on a top lawn of *E. coli* BW25113. The blue and orange arrows indicate the predicted

ColM and SalE1B bands, respectively. The uncropped image is included in Supplementary Information file. **D** LC-MS/MS proteomic analysis of the ColM and SalE1B cocktails produced using either PURE CFE or CECFE, confirming the high abundance of both bacteriocins in both cocktails. Protein ranking of all proteins detected is based on the intensity-based absolute quantification (iBAQ). A lower rank is correlated with a higher abundance. The estimated concentration of ColM and SalE1B, given between brackets, is calculated based on the known added concentration of trypsin (0.01 mg/ml). Bars in (B) represent the average and dots the value of three biological replicates ± SD.

their activity as a cocktail against *E. coli*. Colonies appeared within the inhibition zone for individually expressed ColE1 and MccV (Fig. 3D), as previously observed for singly expressed ColM, MccL, and SalE1B (Fig. 2B). Crucially, no colonies were detected within the inhibition zone of the cocktail-treated cultures (Fig. 3D). The capacity of the ColE1 + MccV cocktail to prevent resistance development was further confirmed with activity assays in liquid cultures (Fig. 3D). Overall, our data demonstrate that our PARAGEN collection can be re-engineered to achieve significantly higher bacteriocin activity and expand the variety of rationally designed bacteriocin cocktails for targeted antimicrobial therapies.

Continuous exchange cell-free expression enhances production of bacteriocin cocktails

Based on the above results, we generated three cocktails (ColM + SalE1B, MccL + SalE1B, and ColE1 + MccV) with similar properties in terms of antibacterial activity and prevention of resistance development. We

arbitrarily choose the cell-free expressed ColM and SalE1B combination for further optimization and characterization. For this purpose, we aimed to scale up (from µl to ml range) and improve the synthesis of this cocktail by using a continuous exchange cell-free expression (CECFE) method (Fig. 4A). CECFE facilitates the continuous flow of energy co-factors, ribonucleotides, and amino acids into the reaction compartment, efficiently removing by-products to increase expression yields. First, we measured the activity of individually and co-expressed ColM and SalE1B bacteriocins produced via the PURE CFE system by spotting the reactions on agar-grown lawns of indicator strains (parental and Keio mutants) (Fig. 4B). This confirmed that the activity of the individual bacteriocins can be specifically traced. More importantly, comparing the cocktail produced via CECFE with the one produced using the PURE CFE system revealed a more than tenfold increase in specific bacteriocin activity with the CECFE method.

Thus far, we validated the activity of each bacteriocin in the cocktails by using bacterial indicator strains that are sensitive to one component but not

the other. To further characterize the ColM + SalE1B cocktail, we demultiplexed the bacteriocins using a direct activity assay with samples fractionated in a Tris-Tricine-SDS page gel (Fig. 4C). This revealed that bacteriocins retain their active linear form and size in the cocktail, as observed in single reactions. The molecular weights of the bacteriocins in both single and combined CFE preparations fall within the predicted range: 29–58 kDa for ColM and SalE1B, respectively.

LC-MS/MS proteomic analysis of the CFE samples further confirmed the identity of the bacteriocins and allowed us to compare the yield of the different CFE preparations. The intensity-based absolute quantification (iBAQ) values indicated that both ColM and SalE1B were highly abundant in all reaction mixtures, highlighting the efficiency of their in vitro production (Fig. 4D and Supplementary Fig. 3a, b). The total protein count in the CECFE reaction was almost seven times higher than that in the PURE system (Fig. 4D and Supplementary Fig. 3a, b). This can be attributed to the composition of the CFE blends: the PURE system relies on a selection of purified *E. coli* proteins, while the CECFE method retains all proteins from lysed *E. coli* cells. Using iBAQ value ratios, the concentration of the bacteriocins in the single and combined CFE reactions was estimated based on the known concentration of trypsin (0.01 mg/ml) added to each sample²⁸ (Fig. 4D and Supplementary Fig. 3a, b). Despite using identical template DNA concentrations, the levels of ColM were several-fold higher compared to those of SalE1B in both single and cocktail CFE reactions. Notably, the estimated concentrations of ColM + SalE1B (in cocktail preparations) were more than 12 and 26 times higher, respectively, in the CECFE reaction (4.58 mg/mL for ColM and 1.20 mg/mL for SalE1B) compared to the PURE CFE (0.36 mg/mL for ColM and 0.05 mg/mL for SalE1B) (Fig. 4D). These concentrations are consistent with the results from the antibacterial activity assays (Fig. 4B) and demonstrate that bacteriocin production can be scaled up by implementing a continuous exchange strategy.

Bacteriocin cocktail to control infections with antibiotic-resistant pathogenic *E. coli* strains in *Galleria mellonella*

The scaling up allowed us to test the efficacy of the ColM + SalE1B cocktail for treating infections of clinical *E. coli* isolates in the animal model *Galleria mellonella*. First, we determined the toxicity of the cocktail prepared using CECFE and observed that 10² and 10³ dilutions did not kill and were less harmful to *G. mellonella* larvae than a more concentrated solution (Fig. 5A, B).

We proceeded to test the efficacy in vitro of the 100-fold diluted ColM + SalE1B cocktail against multidrug-resistant clinical *E. coli* isolates. These strains produce different β -lactamases, such as AmpC and others with extended-spectrum, including CMY-2, SHV-11, CTX-M-14, CTX-M-15, and KPC, NDM, OXA-48 carbapenemases. We observed that the ColM + SalE1B cocktail exhibited varying levels of activity against the clinical strains, ranging from higher to a complete lack of killing activity when compared to its effect on the laboratory strain DH10B. (Supplementary Fig. 4a).

We further assessed the pathogenicity of these clinical isolates against *G. mellonella*. The selected strains lead to sickness and mortality within 24 h post-infection (Fig. 5C and Supplementary Fig. 4b). Importantly, the ColM + SalE1B cocktail proved to be an effective treatment for several isolates, including strains 141, 425, and 10276-2, as it maintained survival rates and health scores comparable to those of control larvae treated with a saline solution. For other strains, the treatment resulted in reduced survival and health score compared to the control population. However, these outcomes were still significantly better compared to untreated larvae (Fig. 5C and Supplementary Fig. 3b). Altogether, our results demonstrate that our bacteriocin synthesis approach facilitates testing the therapeutic potential of alternative antimicrobial combinations.

Multiplexed CFE of bacteriocin cocktails expands antimicrobial activity

Considering the narrower specificity of bacteriocins compared to conventional antibiotics, we aimed to expand the spectrum of activity of bacteriocin therapies by producing cocktails that target different bacterial species. First,

we co-expressed SalE1B with either linear or circular bacteriocins that are active against Gram-positive bacteria (EntL50A or GarML, respectively) (Table 1 and Fig. 6A). The antimicrobial efficacy of these cocktails was assessed on lawns of both Gram-negative and Gram-positive bacteria (*E. coli* DH10B and *Pediococcus pentosaceus* CWBI B29, respectively). Individual bacteriocin synthesis reactions only showed activity against their expected bacterial targets (Fig. 6B). Notably, both *E. coli* and *P. pentosaceus* strains were effectively cleared when bacteriocins were co-expressed (Fig. 6B). These results demonstrate that bacteriocin cocktails can effectively expand the spectrum of antimicrobial activity. These findings also show that antimicrobial CFE can be multiplexed to produce cocktails with both unmodified and modified bacteriocins.

CFE of bacteriocin cocktails can be further multiplexed

To further challenge the synthesis of bacteriocin cocktails, we tested whether adding a third DNA template would compromise expression efficiency of a cocktail containing EntL50A and SalE1B (Fig. 7A). As a proxy for expression competition, we measured GFP fluorescence over time in a cocktail preparation and observed that GFP expression reached a lower plateau in reactions co-expressed with EntL50A + SalE1B, compared to single GFP synthesis reactions. Nevertheless, spot assays on indicator strains showed that the bacteriocins retained their activity after several dilutions, when co-expressed with GFP (Fig. 7B). Thus, it is possible to co-express cocktails of more than two bacteriocins.

To evaluate whether three bacteriocins can be co-expressed, we synthesized a cocktail with SalE1B + ColM + MccL, using *E. coli* strains as indicators to distinguish the activity of each bacteriocin. First, we constructed *E. coli* strains with defined resistance profiles to specifically detect (demultiplex) the activity of each bacteriocin in the cocktail. To assess ColM activity, we selected a $\Delta cirA$ strain (already resistant to MccL), which is resistant to SalE1B. To isolate the activity of SalE1B, we employed a *tonB* mutant, which is resistant to both ColM and MccL. Finally, to detect MccL, we used a resistant isolate (mutant #2) selected after exposure to SalE1B, which carries mutations in *fluA* and *tolQ*, rendering it resistant to both ColM and SalE1B (Supplementary Table 1 and Supplementary Fig. 2). Activity assays with serial dilutions on these indicator strains confirmed the functionality of each component in a multiplexed cocktail with three bacteriocins and demonstrated that such combinations can be produced using CFE in a fast and robust manner (Fig. 7C).

Discussion

In this study, we demonstrated that applying engineering and synthetic biology principles, such as standardization, optimization, and multiplexing, can enable the fast, robust, and customized synthesis of combination therapies for combating pathogenic and antibiotic-resistant bacteria. By leveraging genetic devices from the PARAGEN collection, we developed a platform for the in vitro co-expression of bacteriocins with diverse sizes and structures. We validated the individual activity of the bacteriocins in the cocktails using electrophoretic separation under non-denaturing conditions, proteomic analysis, and testing their activity against strains that are sensitive to each bacteriocin specifically. The processes of multiplexing (co-expression of bacteriocins) and demultiplexing (validation of each bacteriocin synthesised) in this research offer an alternative solution to preparations of cocktails using mixtures of bacteriocins expressed independently. Our approach allows for testing bacteriocin combinations, while reducing time, labour, and costs of preparation. Such efficiency is particularly advantageous when rapid prototyping or high-throughput screening is required²⁹.

Importantly, we showed that bacteriocin combinations co-expressed in single CFE reactions can enhance bactericidal activity, expand the spectrum of targets, and prevent the emergence of AMR. Additionally, an iterative Design-Build-Test-Learn cycle allowed us to refine the PARAGEN collection further, incorporating post-translational additives, such as a DSB enhancer blend, to increase bacteriocin production. Finally, our CECFE approach enabled us to scale up bacteriocin cocktail synthesis and facilitated

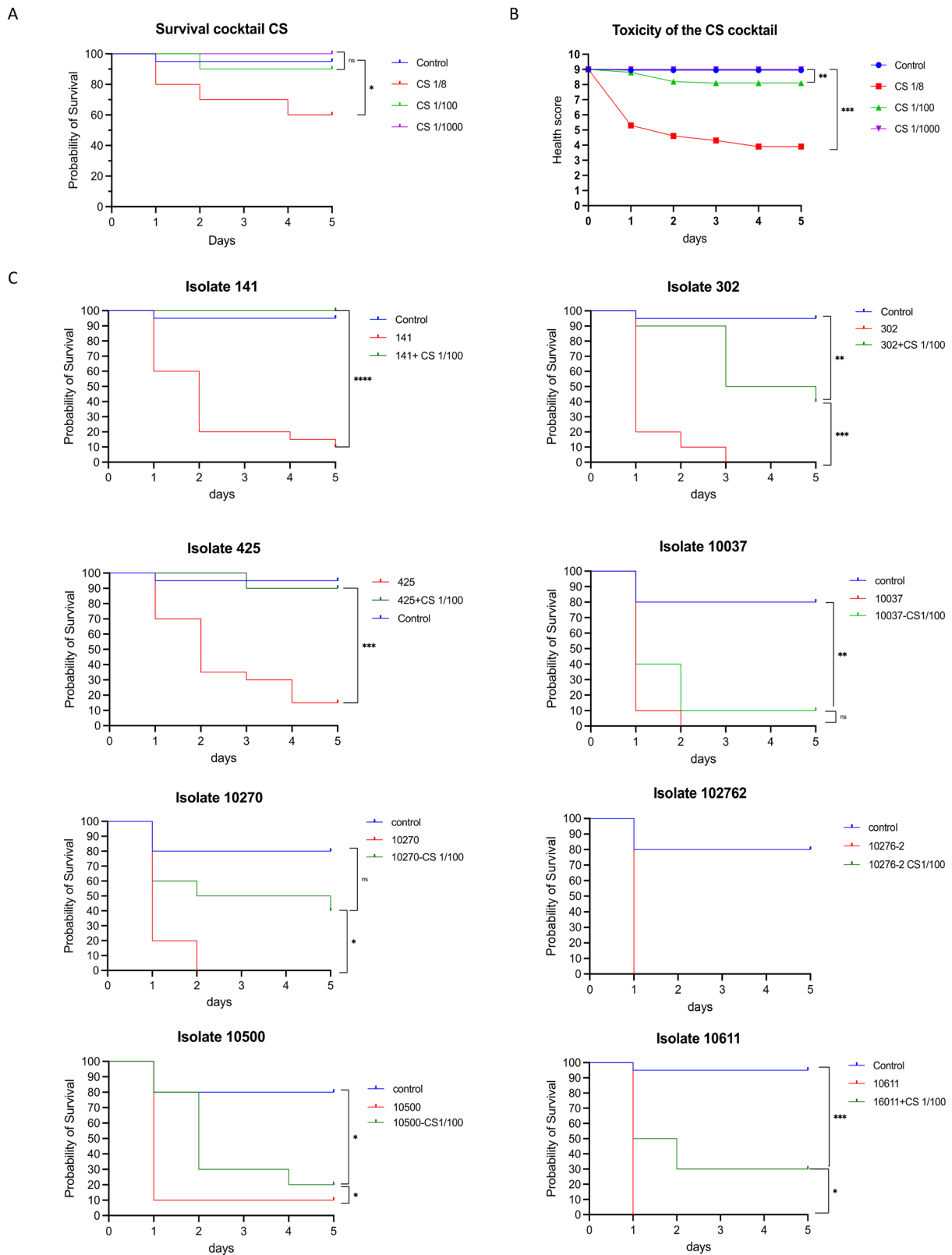


Fig. 5 | Diluted bacteriocin cocktail is not toxic and improves survival of *Galleria mellonella* after bacterial infection. A, B Survival (A) and health (B) scores measurements on the animal model *G. mellonella* individuals after injection of different dilutions (1:8, 1:100, and 1:1000) of the ColM + SalE1B cocktail (C + S) produced by CECFE. C Survival score measurements on *G. mellonella* after infection with

antibiotic multi-resistant *E. coli* strains (141, 302, 425, 10037, 10270, 10276-2, 10500, 10611). Blue line in graph for treatment with isolate 10276-2 is superimposed on green one. $n = 10$ per treatment, ns not significantly different ($p \geq 0.05$), * $p < 0.05$, ** $p < 0.01$ and *** $p < 0.001$. Statistical differences in survival rates were calculated using the Log-rank and Wilcoxon tests, with a significance level of $p < 0.05$.

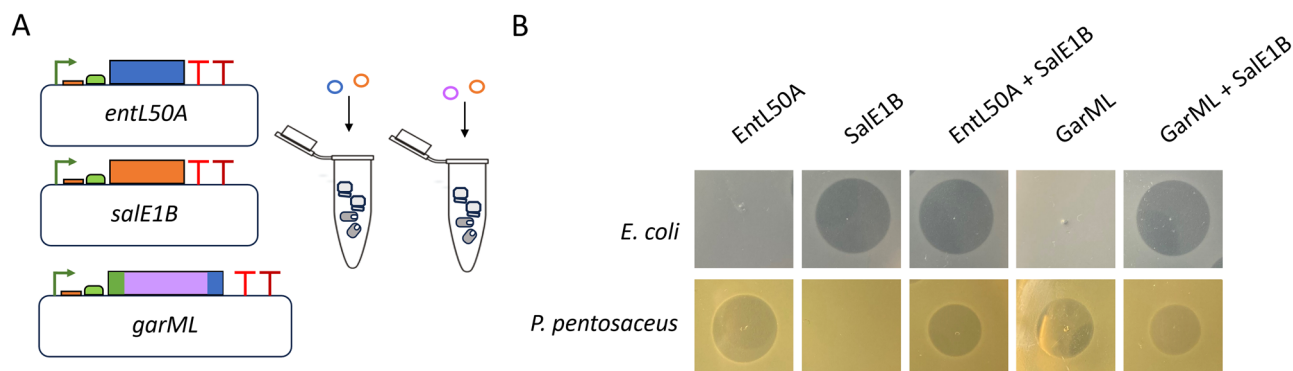


Fig. 6 | Cell-free co-expression of bacteriocins from PARAGEN targeting Gram-positive and -negative bacteria. **A** Bacteriocin gene expression devices from the PARAGEN collection optimized for CFE of either EntL50A, SalE1B, or GarML. **B** Bacteriocin activity tests on *E. coli* DH10B and *P. pentosaceus* CWBI-B29. Cocktails of EntL50A + SalE1B and GarML + SalE1B were synthesized using PURE CFE (PurExpress, NEB).

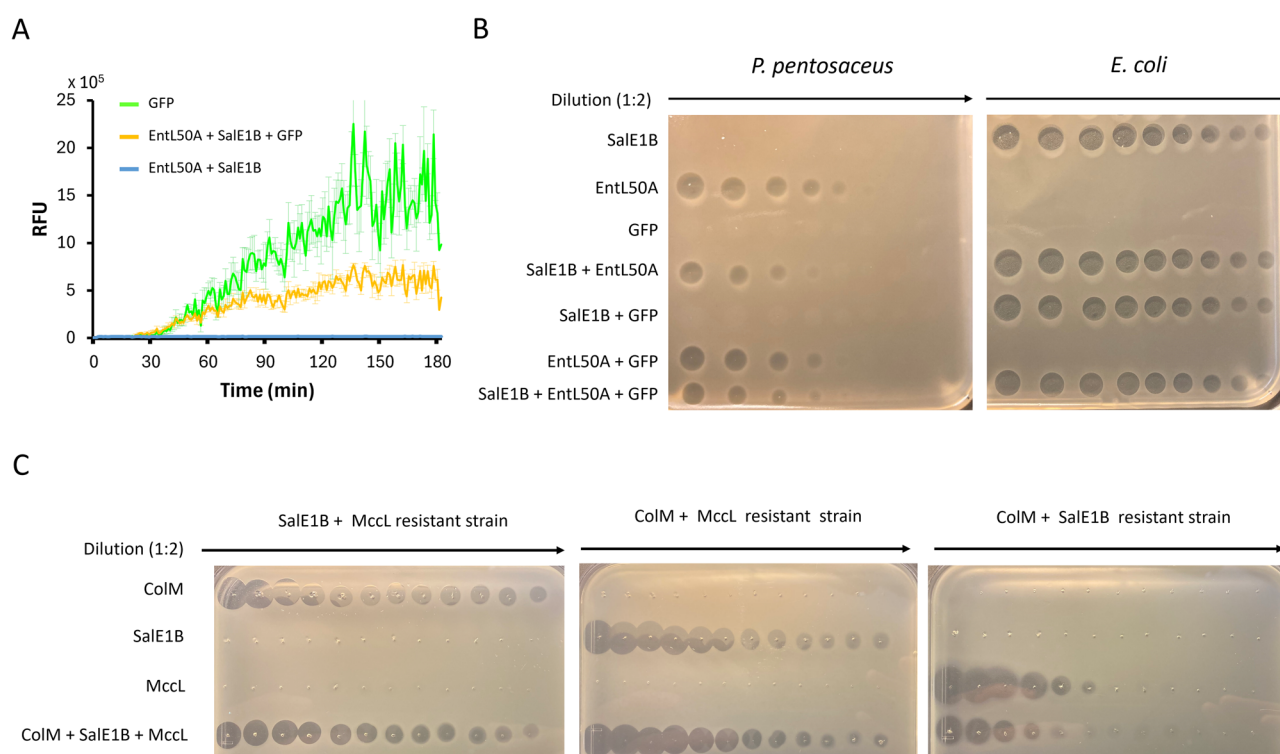


Fig. 7 | Co-expression and bacteriocin activity in combinations with three different DNA molecules. **A** GFP fluorescence (RFU) throughout time in single and combined CFE. Lines represent the average value of three technical replicates and error bars (\pm SD). **B** Bacteriocin activity tests on *E. coli* DH10B and *P. pentosaceus* CWBI-B29. **C** ColM + SalE1B + MccL bacteriocin cocktail activity tests on *E. coli* BW23115 mutants insensitive to two of the three bacteriocins. **A–C** All proteins were synthesized using PURE CFE (PurExpress, NEB).

the use of diluted CFE solutions for infection control with minimal toxicity in an animal model. Altogether, our work serves as a proof of concept, illustrating that complex bacteriocin combinations can be synthesized and tailored to target difficult-to-treat bacterial infections.

Our results showed that the SalE1B + ColM, MccL + SalE1B, Cole1 + MccV cocktails had superior killing activity and AMR prevention compared to single bacteriocin treatments. Importantly, our sequencing data on SalE1B resistant isolates revealed that mutations in a non-cognate receptor gene (*fhuA*). This indicates that, as observed with antibiotics, bacteriocin resistance can appear in the absence of selective pressure^{30,31} and supports the notion that rationally designed combinatorial therapies should be implemented to kill bacteria rapidly, before resistance emerges. Indeed, unlike monotherapy with single antibiotics, cocktails can yield synergistic effects, rejuvenate old antibiotics, minimize resistance development and

toxicity, and expand the spectrum of activity to tackle community-acquired infections^{14,32,33}. This is particularly important given the increasing threat of AMR and the limited discovery and availability of new antibiotics.

In this study, we also synthesized a combination of three bacteriocins, demultiplexed the activity of each individual component and assessed the burden of co-expressing three distinct proteins (two bacteriocins and GFP) in CFE. Although bacteriocin activity was retained when bacteriocin synthesis was further multiplexed, it is important to note that increasing the number of antimicrobials in a cocktail does not necessarily improve bacterial control. The combination of multiple agents can result in antagonistic interactions or reduced antibacterial efficacy³⁴. Furthermore, the development of complex cocktails poses additional challenges as a therapeutic alternative, since each antimicrobial agent must exhibit comparable therapeutic levels and stability over time³⁵.

There is also an important challenge in expressing multiple bacteriocins and controlling the expression levels of each individual component in a reaction. Despite using equimolar concentrations of DNA templates for ColM and SalE1B expression, higher expression levels of ColM were observed in both individual and multiplexed CFE reactions (Supplementary Fig. 3 and Fig. 4D). This difference likely stems from intrinsic properties of the gene sequences and encoded proteins, which can influence expression at multiple levels. Variability in codon usage, mRNA secondary structure, and translation efficiency can all affect protein yield, even under identical transcription and translation conditions^{36–38}. Additionally, SalE1B may be more prone to misfolding or proteolytic degradation in the CFE system, which could further reduce its detectable concentration. Such disparities are well documented in cell-free systems, where co-expression of multiple genes often results in unequal protein output, despite equivalent DNA input³⁹. These findings highlight the importance of further engineering CFE to optimize and control bacteriocin synthesis for multiplexed expression.

We demonstrated the *in vivo* efficacy of a bacteriocin cocktail against highly resistant pathogenic *E. coli* strains carrying critical resistance genes, including *CTX-M-15*, *OXA-48*, *KPC*, and *NDM*. Although our *in vivo* model, *Galleria mellonella*, is not the most closely related to human biology, it offers valuable insights into the potential of bacteriocins as novel antimicrobial therapies. *G. mellonella* has a short reproductive cycle and lower technical and ethical demands compared to vertebrate models, while retaining native immune system functions⁴⁰. These initial findings in our model support further development of targeted bacteriocin cocktails as adjuvants to antibiotic therapies and for the decolonization of resistant strains in more complex infection models. Indeed, the use of *G. mellonella* in preclinical studies has increased in recent years, including in research evaluating the efficacy of the bacteriocin Microbisporicin (NAI-107)^{41,42}. Future studies could investigate the synergistic effects of these bacteriocin cocktails in *G. mellonella* when combined with antibiotics, disinfectants, or antibiofilm agents to better understand their clinical applicability.

It is likely that future cell-free expressed antimicrobial combinations will include bacteriocins other than linear and circular ones. Recently, the CFE of Salivaricin B, a class I bacteriocin with post-translational modifications, was achieved via the co-expression of three distinct DNA templates encoding the precursor, modification, and maturation proteins⁴³. Although our work here focused on bacteriocins with circular and linear structures expressed from single gene parts, future antimicrobial cocktails will likely integrate CFE bacteriocins with more complex structures. It is even conceivable that CFE could facilitate the co-production of bacteriocins with other antimicrobial proteins or agents within a single reaction. Indeed, the *in vitro* co-expression of enzymes for synthesising antimicrobial non-ribosomal peptides, as well as the assembly of phages, has been achieved^{44,45}. The integration of engineering and synthetic biology in the design and synthesis of bacteriocin cocktails thus holds great promise for the development of innovative, precise therapies against multidrug-resistant pathogens.

Methods

Cell-free bacteriocin synthesis

In vitro bacteriocin synthesis was performed using pDNA from the PARAGEN collection⁶⁷ (Table 1) with PurExpress (New England BioLabs) (PURE CFE system) and RTS 500 ProteoMaster *E. coli* HY (biotechrabbit) for CECFE. The RTS ProteoMaster Instrument (Roche) was used for incubation and mixing of the CECFE reactions. Synthesis conditions were followed according to each manufacturer's recommendations. For Garvicin ML production, plasmid pCirc-Npu-GarML was used as template. This plasmid includes the GarML mature sequence flanked by the C- and N-terminal fragments from the *Nostoc punctiforme* (Npu) DnaE split-intein for the circularization of the bacteriocin with the split-intein-mediated ligation (SIML) system⁷. pDNAs for CFE of 2 or 3 bacteriocins, or 2 bacteriocins and GFP; in single reactions were mixed in 1:1 or 1:1:1 ratio of concentrations, using the same concentration for single bacteriocin synthesis.

Optimization of cell-free bacteriocin synthesis

Bacteriocin expression devices from the PARAGEN collection were optimized following template DNA design guidelines for CFE with PURExpress (GeneFrontier Corporation). Our DNA templates were redesigned considering codon usage, AT content after the start codon, and removal of mRNA secondary structures and sequences likely causing frameshift during elongation. In addition, a *lac* operator sequence downstream of the T7 promoter was removed. The sequences for ColE1, GFP, and MccV expression before and after optimization have been shared as Supplementary Information to provide detailed information.

Bacterial growth conditions and strains

E. coli cells were grown at 37 °C for 6–16 h in either LB or Mueller-Hinton medium, as specified. *P. pentosaceus* CWBI B29 cells were grown in MRS media for 18–24 h at 30 °C. *E. coli* strains with mutations for the different bacteriocin receptors were obtained from the Keio collection²⁴. Growth assays in liquid cultures were done in 96-well plates. OD₆₀₀ reads were taken every minute for 48 h using a SpectraMax i3X plate reader at 37 °C with linear shaking before each timepoint.

Bacteriocin activity tests

The activity of bacteriocins was tested on plates and liquid cultures. On solid media, 2.5 µl taken either directly from the cell-free reactions or serial dilutions were prepared and spotted on plates with indicator strains. Plates were prepared by mixing fresh overnight cultures of either *E. coli* or *P. pentosaceus*, normalized to 1.0 OD₆₀₀ with 0.7% agar in a 1:80 and 1:10 ratio, respectively, and pouring the mix on solid growth media (1.5% agar). Bacteriocin spots on bacterial lawns were allowed to dry before incubation.

In liquid media, fresh seed cultures were diluted to 0.1 OD₆₀₀ and the bacteriocin cell-free reactions were diluted 8 times (1:8). Then, 198 µl of the diluted culture was mixed with 2 µl of the diluted bacteriocins in 96-well plates, incubated, and assessed for optical density as indicated above. CFU counts for viability test were done similarly, except that incubation was done using an orbital shaking incubator and samples were taken every hour.

The bacteriocin activity on *E. coli* clinical isolates was evaluated using Mueller-Hinton agar plates (BD, USA) from pure cultures of each strain, in accordance with the EUCAST (European Committee on Antimicrobial Susceptibility Testing) guidelines for antimicrobial susceptibility testing by disc diffusion. A 2.5 µL spot of each bacteriocin was applied directly onto plates inoculated with a 0.5 McFarland suspension of a pure overnight culture strain. The diameter of the inhibition zones around each spot was measured after 24 h of incubation at 35 °C in an aerobic atmosphere.

MIDP determination

MIDP is defined by the lowest dilution showing antimicrobial activity on plates with bacterial lawns. To avoid any bias in determining the MIDP, especially when the inhibition halos become faint, we developed a custom Python script to automatically recognize and analyse these halos from plate images. The script identifies halos by detecting circular areas with a radius greater than 7 pixels and a pixel intensity value that is at least 5 units lower than the background pixel intensity. After testing and iterating with our image set, we found that setting the intensity difference parameter (x) to 5 provided the best balance between sensitivity and specificity.

Fluorescence measurements

GFP fluorescence during cell-free expression was performed using 25 µl reactions with PurExpress (New England BioLabs) in 384-well black microplates, with flat bottoms. Fluorescence readings were taken using a SpectraMax i3x (Molecular Devices) with 485- and 535-nm excitation and emission wavelengths, respectively, at 30 °C after 2.5 h of incubation or through time (every 30 s).

Genome sequencing

gDNA sequencing was performed with a MinION portable sequencing device (Oxford Nanopore). Briefly, gDNA samples were barcoded using a

native barcoding kit 24 V14 (Oxford Nanopore), and samples were loaded into a MinION flow cell (R10.4.1) following manufacturer's instructions. Pod5 data were basecalled with dorado 0.7.3 with dna_r10.4.1_e8.2_400bps_sup@v5.0.0 model to generate fastq files. After basecalling, low-quality reads (< Q12) were removed using Chopper⁴⁶ and filtered reads were used as input to Breseq⁴⁷ with default parameters to identify genomic mutations.

Tris-tricine-SDS Page

CFE reactions containing bacteriocins were mixed with Laemmli sample buffer (33 mM Tris-HCl, pH 6.8, 13% glycerol, 2.1% SDS, 0.01% bromophenol blue) without DTT, directly loaded into a precast Tris-Tricine-SDS gel 16% polyacrylamide (Invitrogen) and run with Tris-MOPS-SDS running buffer (GenScript). After migration, gels were fixed in a solution of 10% acetic acid and 20% propanol, with agitation for 1 h. The gel was washed with agitation, first with 70% ethanol, a second time with 30% ethanol and the last two washes with Mili-Q water, 1 h for each step. The washed gel was placed on top of dry LB solid (1.5% agar) media in a square petri plate. A 600 µl sample from overnight cultured bacteria was mixed with LB solid media to complete 8 ml, then, poured on the LB solid plate with the gel and incubated overnight. Pictures were taken after incubation.

Proteomic analysis of bacteriocin CFE samples

The sample preparation was performed by diluting the CFE reactions containing bacteriocins twice with buffer (10% SDS and 100 mM triethylammonium bicarbonate (TEAB) at pH 8.5) and tip sonicating (3×, 10 s) on ice. After centrifugation for 15 min at max speed, the proteins were reduced and alkylated by adding 10 mM Tris-(2-carboxyethyl)phosphine (TCEP) and 40 mM chloroacetamide, followed by incubation (10 min, 95 °C, 750 rpm) in the dark. The protein concentration was determined via a BCA protein assay and 50 µg of protein was taken. The volumes were adjusted to 50 µl by adding 5% SDS, 50 mM Tri-ethyl-borane and phosphoric acid to a final concentration of 1.2%. Next, the samples were diluted sevenfold using binding buffer (90% methanol in 100 mM TEAB at pH 7.55). Subsequently, the samples were loaded in parts of 400 µL on an S-TrapTM 96-well plate (ProtiFi), positioned on top of a DeepWell plate and centrifuged (2 min, 1500 × g, room temperature). The S-TrapTM plate was washed three times by adding 200 µl binding buffer and centrifuged (2 min, 1500 × g, room temperature). Next, a new DeepWell plate was positioned underneath the S-TrapTM plate and 125 µl 50 mM TEAB containing 1 µg trypsin was added for digestion overnight at 37 °C. Using centrifugation (2 min, 1500 × g, room temperature), peptides were eluted in three steps, first with 80 µl 50 mM TEAB, next with 80 µl 0.2% formic acid (FA) in water, and finally with 80 µl 0.2% FA in 50:50 water/acetonitrile (ACN). The eluted peptides were dried by vacuum centrifugation and re-dissolved in 0.1% trifluoroacetic acid (TFA) in 98:2 water/ACN for an additional purification step on Omix C18 tips (Agilent). Purified samples were vacuum-dried.

For LC-MS/MS analysis, the peptides were re-dissolved in 20 µl loading solvent A (0.1% TFA in 98:2 water/ACN) of which 2 µl was injected for LC-MS/MS analysis on an Ultimate 3000 RSLC nano-LC (Thermo Fisher Scientific, Bremen, Germany) in-line connected to a Q Exactive mass spectrometer (Thermo Fisher Scientific). The samples were flushed through a 5 mm trapping column (Pepmap Neo, 100 µm internal diameter, 5 µm beads, C18, Thermo Fisher Scientific), followed by separation on a 50 cm µPACTM column with C18-encapped functionality (Pharmafluidics, Belgium) kept at a constant temperature of 50 °C. For elution of the peptides, a stepwise gradient was used from 98% solvent A' (0.1% FA in water) to 33% solvent B' (0.1% FA in 20:80 water:ACN) in 28 min up to 55% solvent B' in 15 min followed by a 2 min wash reaching 70% solvent B'. This elution was performed with a stepwise flow rate starting from 750 nl/min for 9 min to 300 nl/min till the end of the run.

The mass spectrometer was operated in data-dependent positive ionization mode while automatically switching between MS and MS/MS acquisition for the 5 most abundant peaks in a given MS spectrum. Therefore, one MS1 scan (m/z 400–2000, AGC target 3×10^6 ions,

maximum ion injection time of 80 msec), acquired at a resolution of 70,000 (at 200 m/z), was followed by up to 5 tandem MS scans (resolution 17,500 at 200 m/z) of the most intense ions fulfilling predefined selection criteria (AGC target 50,000 ions, maximum ion injection time of 80 msec, isolation window of 2 Da, fixed first mass of 140 m/z, spectrum data type: centroid, intensity threshold of 1.3×10^4 , exclusion of unassigned, 1, 5–8, >8 positively charged precursors, peptide match preferred, exclude isotopes 'on', dynamic exclusion time of 12 s). Moreover, the source voltage was set to 3 kV and the capillary temperature to 275 °C. The HCD collision energy was 25% Normalized Collision Energy and internal calibration (lock mass) was performed using the polydimethylcyclsiloxane background ion at 445.120025 Da. Qcloud was implemented to control the instrument's longitudinal performance⁴⁸.

For data analysis, the MaxQuant algorithm (version 2.5.0.0) was used to search LC-MS/MS runs of all samples separately, by implementing mainly default search settings, including a false discovery rate set at 1% on peptide and protein level. The spectra were searched against the reference Swiss-Prot (release version 2024_09) proteome database UP000291778 containing 5190 *E. coli* protein sequences, supplemented with the amino acid sequences of ColM and SalE1B. During the main search, the mass tolerances for precursor- and fragment ions were set to 4.5 and 20 ppm, respectively. The enzyme specificity was set to the C-terminus of arginine and lysine, while also allowing cleavage at Arg/Lys-Pro bonds with a maximum of two missed cleavages. As variable modifications, oxidation of methionine residues and acetylation of protein N-termini were implemented, while carbamidomethylation of cysteine residues was applied as a fixed modification. For all samples, S-curves were generated by plotting the log₂ transformation of the iBAQ intensity values from each detected protein against their protein ranks. From these plots, the ratio of ColM and SalE1B to trypsin was determined. Next, the concentrations of both bacteriocins were estimated by considering these ratios and the known concentration of trypsin (0.01 mg/ml).

Toxicity and bacteriocin activity in *Galleria mellonella*

Adult larvae of *Galleria mellonella* (TerraMania, Arnhem, Netherlands) were used for the infection model. Upon arrival, the larvae were stored at room temperature and used within three days. Healthy, non-discolored larvae weighing approximately 0.30 g were selected for analysis^{41,42,49}. After the selection of larvae for each experimental group, all individuals, data points and results were included in the analysis. The infected inoculum was prepared from an overnight pure culture on Columbia 5% sheep blood agar (Becton Dickinson, USA) and adjusted for each isolate to 10⁶ to 10⁸ CFU/mL to achieve 50% to 80% mortality within 48 h. Larvae were inoculated by injecting a 10 µl aliquot into the hemocoel via the last left proleg using sterile 0.3 mL U100 insulin syringes (BD Micro-Fine) with a Microinjector (KDS 100 automated syringe pump, KD Scientific), followed by a 10 µl treatment or sterile saline serum injection (Mini-Plasco B. Braun NaCl 0.9%) 15 min later on the right side. In each experiment, a group receiving two saline serum injections and another receiving the bacteriocin solution, followed by a saline serum injection were used as negative and toxicity control groups, respectively. The insects were incubated in sterile Petri dishes, kept in the dark at 37 °C in atmospheric air, and observed every 24 h for 5 days. Health scores were calculated daily according to the health index score system⁴⁰, and larvae were considered dead if they did not respond to touch stimuli.

Statistics and reproducibility

Bacteriocin activity assays in vitro, in liquid media, and to determine MIDP on solid media, were performed using three biologically independent replicates. Numerical data for bacteriocin in vitro activity assays represent the mean values of three replicates ± standard deviations. In vivo bacteriocin efficacy and toxicity assays were performed using 10 larvae per treatment and controls^{41,42,49}. Randomization, confounding variables and humane endpoints were not considered in the experiments. Survival curves were plotted using the Kaplan–Meier method in GraphPad Prism 10. ns: not significantly different ($p \geq 0.05$), * $p < 0.05$, ** $p < 0.01$ and *** $p < 0.001$.

Statistical differences in survival rates were calculated using the Log-rank and Wilcoxon tests, with a significance level of $p < 0.05$.

Reporting summary

Further information on research design is available in the Nature Portfolio Reporting Summary linked to this article.

Data availability

The main data supporting the findings of this study, as well as protocols, are available within the article and its Supplementary Information. Nanopore reads for this study have been deposited in the Sequence Read Archive (SRA) at National Center for Biotechnology Information (NCBI) under accession number PRJNA1218925. All source data can be obtained in the Supplementary Data files (Supplementary Data 1–12).

Received: 15 January 2025; Accepted: 31 July 2025;

Published online: 19 August 2025

References

- Cotter, P. D., Ross, R. P. & Hill, C. Bacteriocins—a viable alternative to antibiotics?. *Nat. Rev. Microbiol.* **11**, 95–105 (2013).
- Heilbronner, S., Krismer, B., Brötz-Oesterhelt, H. & Peschel, A. The microbiome-shaping roles of bacteriocins. *Nat. Rev. Microbiol.* **19**, 726–739 (2021).
- Guinane, C. M. et al. The bacteriocin bactofencin A subtly modulates gut microbial populations. *Anaerobe* **40**, 41–49 (2016).
- Rea, M. C. et al. Effect of broad- and narrow-spectrum antimicrobials on *Clostridium difficile* and microbial diversity in a model of the distal colon. *Proc. Natl. Acad. Sci. USA* **108**, 4639–4644 (2011).
- Gebhart, D. et al. A modified R-type bacteriocin specifically targeting *Clostridium difficile* prevents colonization of mice without affecting gut microbiota diversity. *mBio* **6**, e0001128 (2015).
- Gabant, P. & Borrero, J. PARAGEN 1.0: a standardized synthetic gene library for fast cell-free bacteriocin synthesis. *Front. Bioeng. Biotechnol.* **7**, 213 (2019).
- Peña, N. et al. In vitro and in vivo production and split-intein mediated ligation (SIML) of circular bacteriocins. *Front. Microbiol.* **13**, 1052686 (2022).
- Jaumaux, F. et al. Selective bacteriocins: a promising treatment for *Staphylococcus aureus* skin infections reveals insights into resistant mutants, vancomycin resistance, and cell wall alterations. *Antibiotics* **12**, 947 (2023).
- Damoczi, J. et al. Uncovering the arsenal of class II bacteriocins in *salivarius* streptococci. *Commun. Biol.* **7**, 1511 (2024).
- Pandi, A. et al. Cell-free biosynthesis combined with deep learning accelerates de novo development of antimicrobial peptides. *Nat. Commun.* **14**, 7197 (2023).
- Fedorec, A. J., Karkaria, B. D., Sulu, M. & Barnes, C. P. Single strain control of microbial consortia. *Nat. Commun.* **12**, 1977 (2021).
- Rutter, J. W. et al. A bacteriocin expression platform for targeting pathogenic bacterial species. *Nat. Commun.* **15**, 6332 (2024).
- Bartram, E., Asai, M., Gabant, P. & Wigneshweraraj, S. Enhancing the antibacterial function of probiotic *Escherichia coli* Nissle: when less is more. *Appl. Environ. Microbiol.* **89**, e00975–23 (2023).
- Coates, A. R., Hu, Y., Holt, J. & Yeh, P. Antibiotic combination therapy against resistant bacterial infections: synergy, rejuvenation and resistance reduction. *Expert Rev. Anti. Infect. Ther.* **18**, 5–15 (2020).
- Martin, A., Bland, M. J., Rodriguez-Villalobos, H., Gala, J. L. & Gabant, P. Promising antimicrobial activity and synergy of bacteriocins against *Mycobacterium tuberculosis*. *Microb. Drug Resist.* **29**, 165–174 (2023).
- Mathur, H. et al. Bacteriocin-antimicrobial synergy: a medical and food perspective. *Front. Microbiol.* **8**, 1205 (2017).
- Rendueles, C. et al. Combined use of bacteriocins and bacteriophages as food biopreservatives: a review. *Int. J. Food Microbiol.* **368**, 109611 (2022).
- Vijayakumar, P. P. & Muriana, P. M. Inhibition of *Listeria monocytogenes* on ready-to-eat meats using bacteriocin mixtures based on mode of action. *Foods* **6**, 22 (2017).
- Kranjec, C. et al. A bacteriocin-based treatment option for *Staphylococcus haemolyticus* biofilms. *Sci. Rep.* **11**, 13909 (2021).
- Guzmán, F., Barberis, S. & Illanes, A. Peptide synthesis: chemical or enzymatic. *Electron. J. Biotechnol.* **10**, 279–314 (2007).
- Garenne, D. et al. Cell-free gene expression. *Nat. Rev. Methods Prim.* **1**, 49 (2021).
- Gillor, O., Kirkup, B. C. & Riley, M. A. Colicins and microcins: the next generation antimicrobials. *Adv. Appl. Microbiol.* **54**, 129–146 (2004).
- Schneider, T. et al. Plant-made *Salmonella* bacteriocins salmocins for control of *Salmonella* pathogens. *Sci. Rep.* **8**, 4078 (2018).
- Baba, T. et al. Construction of *Escherichia coli* K-12 in-frame, single-gene knockout mutants: the Keio collection. *Mol. Syst. Biol.* **2**, 2006.0008 (2006).
- Telhig, S., Ben Said, L., Zirah, S., Fliss, I. & Rebuffat, S. Bacteriocins to thwart bacterial resistance in Gram-negative bacteria. *Front. Microbiol.* **11**, 586433 (2020).
- Jew, K. et al. Characterizing and improving pET vectors for cell-free expression. *Front. Bioeng. Biotechnol.* **10**, 895069 (2022).
- Håvarstein, L. S., Holo, H. & Nes, I. F. The leader peptide of colicin V shares consensus sequences with leader peptides that are common among peptide bacteriocins produced by Gram-positive bacteria. *Microbiology* **140**, 2383–2389 (1994).
- Zhao, M. et al. A comprehensive analysis and annotation of human normal urinary proteome. *Sci. Rep.* **7**, 3024 (2017).
- Yim, S. S. et al. Multiplex transcriptional characterizations across diverse bacterial species using cell-free systems. *Mol. Syst. Biol.* **15**, e8875 (2019).
- Gillespie, S. H. Antibiotic resistance in the absence of selective pressure. *Int. J. Antimicrob. Agents* **17**, 171–176 (2001).
- Knöppel, A., Näsval, J. & Andersson, D. I. Evolution of antibiotic resistance without antibiotic exposure. *Antimicrob. Agents Chemother.* **61**, e01128–17 (2017).
- Drusano, G. L. et al. Analysis of combination drug therapy to develop regimens with shortened duration of treatment for tuberculosis. *PLoS ONE* **9**, e101311 (2014).
- Zhou, A. et al. Synergistic interactions of vancomycin with different antibiotics against *Escherichia coli*: trimethoprim and nitrofurantoin display strong synergies with vancomycin against wild-type *E. coli*. *Antimicrob. Agents Chemother.* **59**, 276–281 (2015).
- Lázár, V., Snitser, O., Barkan, D. & Kishony, R. Antibiotic combinations reduce *Staphylococcus aureus* clearance. *Nature* **610**, 540–546 (2022).
- Tyers, M. & Wright, G. D. Drug combinations: a strategy to extend the life of antibiotics in the 21st century. *Nat. Rev. Microbiol.* **17**, 141–155 (2019).
- Kudla, G., Murray, A. W., Tollervey, D. & Plotkin, J. B. Coding-sequence determinants of gene expression in *Escherichia coli*. *Science* **324**, 255–258 (2009).
- Plotkin, J. B. & Kudla, G. Synonymous but not the same: the causes and consequences of codon bias. *Nat. Rev. Genet.* **12**, 32–42 (2011).
- Espah Borujeni, A., Channarasappa, A. S. & Salis, H. M. Translation rate is controlled by coupled trade-offs between site accessibility, selective RNA unfolding and sliding at upstream standby sites. *Nucleic Acids Res.* **42**, 2646–2659 (2014).
- Caschera, F. & Noireaux, V. A cost-effective polyphosphate-based metabolism fuels an all *E. coli* cell-free expression system. *Metab. Eng.* **27**, 29–37 (2015).

40. Ménard, G., Rouillon, A., Cattoir, V. & Donnio, P. Y. *Galleria mellonella* as a suitable model of bacterial infection: past, present and future. *Front. Cell. Infect. Microbiol.* **11**, 782733 (2021).
 41. Hofkens, N. et al. Microbisporicin (NAI-107) protects *Galleria mellonella* from infection with *Neisseria gonorrhoeae*. *Microbiol. Spectr.* **11**, e02825–23 (2023).
 42. Hofkens, N. et al. Protective effect of microbisporicin (NAI-107) against vancomycin-resistant *Enterococcus faecium* infection in a *Galleria mellonella* model. *Sci. Rep.* **14**, 4786 (2024).
 43. Liu, W. Q. et al. Cell-free biosynthesis and engineering of ribosomally synthesized lanthipeptides. *Nat. Commun.* **15**, 4336 (2024).
 44. Emslander, Q. et al. Cell-free production of personalized therapeutic phages targeting multidrug-resistant bacteria. *Cell Chem. Biol.* **29**, 1434–1445 (2022).
 45. Sword, T. T., Abbas, G. S. & Bailey, C. B. Cell-free protein synthesis for nonribosomal peptide synthetic biology. *Front. Nat. Prod.* **3**, 1353362 (2024).
 46. De Coster, W. & Rademakers, R. NanoPack2: population-scale evaluation of long-read sequencing data. *Bioinformatics* **39**, btad311 (2023).
 47. Deatherage, D. E. & Barrick, J. E. Identification of mutations in laboratory-evolved microbes from next-generation sequencing data using breseq. In *Engineering and Analyzing Multicellular Systems: Methods in Molecular Biology*. (eds Sun, L. Shou, W.) **1151** 165–188 (Humana Press, New York NY, 2014).
 48. Chiva, C. et al. QCloud: a cloud-based quality control system for mass spectrometry-based proteomics laboratories. *PLoS ONE* **13**, e0189209 (2018).
 49. Djokaite, A., Humbert, M. V., Borkowski, E., La Ragione, R. M. & Christodoulides, M. Establishing an invertebrate *Galleria mellonella* greater wax moth larval model of *Neisseria gonorrhoeae* infection. *Virulence* **12**, 1900–1921 (2021).
 50. Cintas, L. M. et al. Biochemical and genetic evidence that *Enterococcus faecium* L50 produces enterocins L50A and L50B, the sec-dependent enterocin P, and a novel bacteriocin secreted without an N-terminal extension termed enterocin Q. *J. Bacteriol.* **182**, 6806–6814 (2000).
- H.G., J.M., P.H.; analysis and interpretation of data. A.Q.Y., H.R.V., H.V.C., H.G., J.M., J.B., P.H., P.G.; draft or revising the manuscript. All authors read and approved the final manuscript

Competing interests

The authors declare the following competing interests: Juan Borrero (JB), Pascal Hols (PH) and Philippe Gabant (PG) declare that they are listed as inventors in the following patents and patent applications related to bacteriocin production and uses: J.B. and P.G., “Bacteriocin polypeptides, nucleic acids encoding same, and methods of use thereof”, Application PCT/US2023/067567; P.G., “Controlled growth of microorganisms”, US Patents 9,333,227/10,188,114/11,427,800/12,297,422 + CN ZL 201480057387.2/ZL 201910882176.7 + EP3035802B1 + BR112016003533-0/1220210154171 + IN389267; P.H.: “Peptides for inducing bacteriocin synthesis and methods to identify and/or select and/or optimize the same”, US Patent 12,234,299. P.H. is a member of the Scientific Advisory Board of the Syngulon company. All other authors declare no competing interests.

Additional information

Supplementary information The online version contains supplementary material available at <https://doi.org/10.1038/s42003-025-08639-y>.

Correspondence and requests for materials should be addressed to Alex Quintero-Yanes or Philippe Gabant.

Peer review information *Communications Biology* thanks Takeshi Zendo and the other, anonymous, reviewer(s) for their contribution to the peer review of this work. Primary Handling Editor: Tobias Goris. A peer review file is available.

Reprints and permissions information is available at <http://www.nature.com/reprints>

Publisher's note Springer Nature remains neutral with regard to jurisdictional claims in published maps and institutional affiliations.

Open Access This article is licensed under a Creative Commons Attribution-NonCommercial-NoDerivatives 4.0 International License, which permits any non-commercial use, sharing, distribution and reproduction in any medium or format, as long as you give appropriate credit to the original author(s) and the source, provide a link to the Creative Commons licence, and indicate if you modified the licensed material. You do not have permission under this licence to share adapted material derived from this article or parts of it. The images or other third party material in this article are included in the article's Creative Commons licence, unless indicated otherwise in a credit line to the material. If material is not included in the article's Creative Commons licence and your intended use is not permitted by statutory regulation or exceeds the permitted use, you will need to obtain permission directly from the copyright holder. To view a copy of this licence, visit <http://creativecommons.org/licenses/by-nc-nd/4.0/>.

© The Author(s) 2025

Acknowledgements

We thank Takashi Ebihara and Tomoko Miyagi from GeneFrontier Corporation for assistance in the optimization of our DNA sequences. The work of A.Q., K.P., O.D.V., and P.G. was funded by SWP Research from the Walloon Region (Grant N° 8723 PROACTIF). H.V.C. was funded by a Research Foundation-Flanders (FWO) S.B. scholarship (1S28323N). H.G. was funded by a Research Foundation-Flanders (FWO) senior postdoctoral fellowship (12A4N25N). J.B. has financial support from the contract (article 83) between Syngulon and the Universidad Complutense de Madrid (SYNGULON, S.A./27-2022) and Fondo Especial de Investigación (FEI) from the Universidad Complutense de Madrid (FEI24/08). P.H. was funded by the Belgian National Fund for Scientific Research (PDR grant T.0111.22) and the Concerted Research Actions (ARC grant 22/27-120) from Federation Wallonia-Brussels. Finally, we thank the VIB Proteomics Core for the proteomic analysis of the bacteriocin cocktails.

Author contributions

A.Q.Y., P.G.; conception and design. A.Q.Y., O.D.V., H.R.V., H.V.C., H.G., J.B.; acquisition of data. K.P.; bioinformatic analysis. A.Q.Y., H.R.V., H.V.C.,